

Atmospheric muon flux expected at the PeV scale

A. A. Kochanov^{*†}, T. S. Sinegovskaya^{*}, S. I. Sinegovsky^{*†},
A. Misaki^{‡§}, N. Takahashi[¶]

^{*} Institute of Applied Physics, Irkutsk State U., Irkutsk, Russia

[†] Depart. of Theor. Physics, Irkutsk State U., Irkutsk, Russia

[‡] Innovative Research Organization, Saitama U., Saitama, Japan

[§] Research Institute for Science and Engineering, Waseda U., Tokyo, Japan

[¶] Graduate School of Science and Technology, Hirosaki U., Hirosaki, Japan

Abstract. In the near future the energy region above few hundreds of TeV may really be accessible for measurements of the atmospheric muon spectrum by the IceCube array. Therefore one expects that muon flux uncertainties above 50 TeV, related to a poor knowledge of charm production cross sections and insufficiently examined primary spectra and composition, will be diminished. We give predictions for the very high-energy muon spectrum at sea level, obtained with the three hadronic interaction models, taking into account also the muon contribution due to decays of the charmed hadrons.

Keywords: cosmic ray muons, high-energy hadronic interactions

I. INTRODUCTION

The atmospheric neutrino flux at high energies is inevitably dominated by the prompt component due to decays of the charmed hadrons (D^\pm , D^0 , \bar{D}^0 , D_s^\pm , Λ_c^\pm , ...), hence the prompt neutrino flux becomes the major source of the background in searches for a diffuse astrophysical neutrino flux [1], [2], [3], [4]. Insufficiently explored processes of the charm production give rise to most uncertainty in muon and neutrino fluxes. IceCube, the first to begin operating as the Km3 neutrino telescope, has the real capability [5] to measure the atmospheric muon spectrum at energies up to 1 PeV and to shed light on the feasible range of the cross sections for the charmed particle production.

In this work we try to extend to higher energies the muon flux calculations basing on the active hadronic interaction models with use of using the most reliable data of the primary cosmic ray measurements. We present results of the conventional muon flux calculations in the range 10–10⁷ GeV using hadronic models QGSJET-II 03 [6], SIBYLL 2.1 [7], EPOS [8] as well as Kimel and Mikhov (KM) [9], that were tested also in recent atmospheric muon flux calculations [10], [11]. At the muon energies $E_\mu \gtrsim 50$ TeV we add the prompt muon flux originating from decays of the charmed hadrons, produced in collisions of cosmic rays with nuclei of air (for review see e.g. [12], [13], [14], [15]).

II. THE METHOD

The high-energy muon fluxes are calculated using the approach [16] to solve the atmospheric hadron cascade equations taking into account non-scaling behavior of inclusive particle production cross-sections, rise of total inelastic hadron-nuclei cross-sections, and the non-power law primary spectrum (see also [11]).

To obtain the differential energy spectra of protons $p(E, h)$ and neutrons $n(E, h)$ at the depth h one needs to solve the set of equations:

$$\frac{\partial N^\pm(E, h)}{\partial h} = -\frac{N^\pm(E, h)}{\lambda_N(E)} + \frac{1}{\lambda_N(E)} \int_0^1 \Phi_{NN}^\pm(E, x) N^\pm(E/x, h) \frac{dx}{x^2}, \quad (1)$$

where $N^\pm(E, h) = p(E, h) \pm n(E, h)$,

$$\Phi_{NN}^\pm(E, x) = \frac{E}{\sigma_{pA}^{in}(E)} \left[\frac{d\sigma_{pp}(E_0, E)}{dE} \pm \frac{d\sigma_{pn}(E_0, E)}{dE} \right],$$

$\lambda_N(E) = 1/[N_0 \sigma_{pA}^{in}(E)]$ is the nucleon interaction length; $x = E/E_0$ is the fraction of energy carried away by the secondary nucleon; $d\sigma_{ab}/dE$ – differential cross sections for inclusive reaction $a + A \rightarrow b + X$. The boundary conditions for Eq. (1) are $N^\pm(E, 0) = p_0(E) \pm n_0(E)$.

Consider that the solution of the system is

$$N^\pm(E, h) = N^\pm(E, 0) \exp \left[-\frac{h(1 - Z_{NN}^\pm(E, h))}{\lambda_N(E)} \right], \quad (2)$$

where $Z_{NN}^\pm(E, h)$ are unknown functions. Substituting Eq. (2) into Eq. (1) we find the equation for these functions Z_{NN}^\pm (Z -factors):

$$\frac{\partial(hZ_{NN}^\pm)}{\partial h} = \int_0^1 \Phi_{NN}^\pm(E, x) \eta_{NN}^\pm(E, x) \times \exp[-tD_{NN}^\pm(E, x, t)] dx, \quad (3)$$

where $\eta_{NN}^\pm(E, x) = x^{-2} N^\pm(E/x, 0)/N^\pm(E, 0)$,

$$D_{NN}^\pm(x, E, t) = \frac{1 - Z_{NN}^\pm(E/x, t)}{\lambda_N(E/x)} - \frac{1 - Z_{NN}^\pm(E, t)}{\lambda_N(E)}.$$

By integrating Eq. (3) we obtain the nonlinear integral equation

$$Z_{NN}^{\pm}(E, h) = \frac{1}{h} \int_0^h dt \int_0^1 dx \Phi_{NN}^{\pm}(E, x) \eta_{NN}^{\pm}(E, x) \times \exp \left[-t D_{NN}^{\pm}(E, x, t) \right], \quad (4)$$

which can be solved by iterations. The simple choice of zero-order approximation is $Z_{NN}^{\pm(0)}(E, h) = 0$, that is $D_{NN}^{\pm(0)}(E, x, h) = 1/\lambda_N(E/x) - 1/\lambda_N(E)$. For the n -th step we find

$$Z_{NN}^{\pm(n)}(E, h) = \frac{1}{h} \int_0^h dt \int_0^1 dx \Phi_{NN}^{\pm}(E, x) \eta_{NN}^{\pm}(E, x) \times \exp \left[-t D_{NN}^{\pm(n-1)}(E, x, t) \right], \quad (5)$$

$$D_{NN}^{\pm(n)}(E, x, h) = \frac{1 - Z_{NN}^{\pm(n)}(E/x, h)}{\lambda_N(E/x)} - \frac{1 - Z_{NN}^{\pm(n)}(E, h)}{\lambda_N(E)}. \quad (6)$$

Nontrivial structure of the nucleon Z -factors (Fig. 1) results from the non-power law behavior of the ATIC-2 primary spectrum (see later), non-scaling behavior of the particle production cross-sections and the energy

dependence of inelastic hadron-nucleus cross-sections. After that, using the obtained nucleon fluxes, we are able to calculate successively the meson and the lepton fluxes [11].

In our calculations we rely on recent data on the primary cosmic ray (PCR) spectra and composition obtained with Advanced Thin Ionization Calorimeter, balloon-borne experiment ATIC-2 [17]. In order to extend the calculations to higher energies, up to 10 PeV, we use the data of the GAMMA experiment [18]. The energy spectra and elemental composition, obtained in the GAMMA experiment, cover the 10^3 – 10^5 TeV range and agree with the corresponding extrapolations of known balloon and satellite data at $E \geq 10^3$ TeV. Alternative primary spectra, used in the calculations for a region of very high energies, is the model by Zatsepin and Sokolskaya (ZS) [19]. The ZS proton spectrum at $E \gtrsim 10^6$ GeV is compatible with KASCADE data [20] and the helium one is within the range of the KASCADE spectrum reconstructed with use of QGSJET 01 and SIBYLL models. Besides we use also the Gaisser and Honda spectra (GH) [21] to compute the muon flux in more narrow energy range $E_{\mu} \lesssim 10^5$ GeV.

III. HIGH-ENERGY MUON SPECTRA

Apart from evident sources of AM, $\pi_{\mu 2}$ and $K_{\mu 2}$ decays, we take into consideration three-particle semileptonic decays, $K_{\mu 3}^{\pm}$, $K_{\mu 3}^0$. Also we take into account small fraction of the muon flux originated from decay chains $K \rightarrow \pi \rightarrow \mu$ ($K_S^0 \rightarrow \pi^+ + \pi^-$, $K^{\pm} \rightarrow \pi^{\pm} + \pi^0$).

The prompt muon contribution due to decays of charmed hadrons at high energies is considered for the three charm production models, the recombination quark-parton model (RQPM) [12], quark-gluon string model QGSM [22], [12], [13], and the model by Pasquali, Reno and Sarcevic (PRS) [23] (see also [15]). Both RQPM and QGSM are the nonperturbative models, whereas PRS is based on the next-to-leading-order QCD calculations.

The high energy spectra of conventional and prompt muons at ground level calculated for the vertical direction are shown in Fig. 2 along with experimental data. The shaded areas here indicate the calculations of the conventional muon flux with KM model for the case of the ATIC-2 primary spectrum (light band on the left) and the GAMMA one (dark band on the right). The size of the bands correspond to statistical errors in the ATIC-2 and GAMMA experiments. Solid, dashed, dash-dotted, and dotted lines indicate the calculations with use of ZS spectrum and set of hadronic models, KM, SIBYLL 2.1, EPOS 1.61, and QGSJET-II. The experimental data comprise the measurements of L3+Cosmic [24], Cosmo-ALEPH [25] as well as the data (converted to the surface) of deep underground experiments MSU [26], MACRO [27], LVD [28], Frejus [29], Baksan [30], Artyomovsk [31]. Notice that the calculation results do not fit well the Frejus and MSU data even though taking

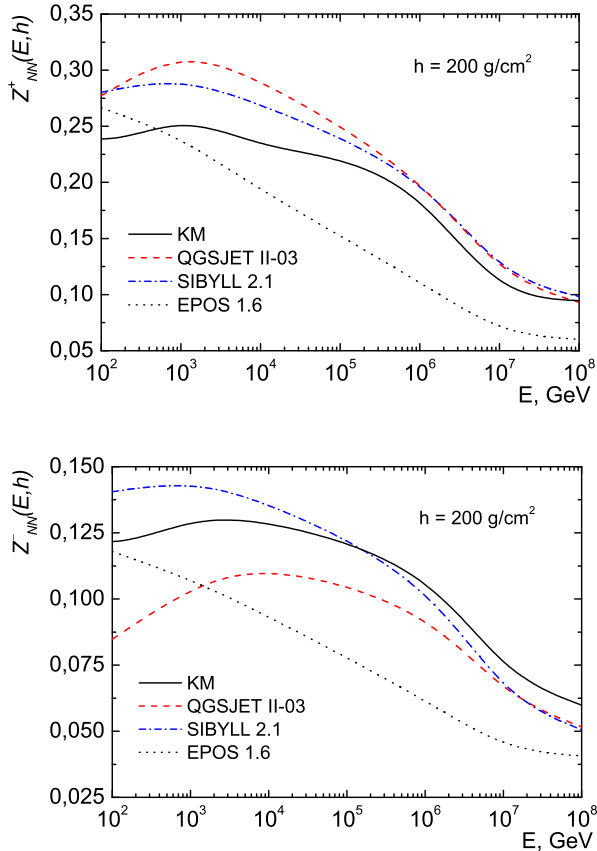


Fig. 1: The energy dependence of $Z_{NN}^{\pm}(E, h)$ -factors at the depth of $200 \text{ g}\cdot\text{cm}^{-2}$ calculated for the ATIC-2 primary spectrum.

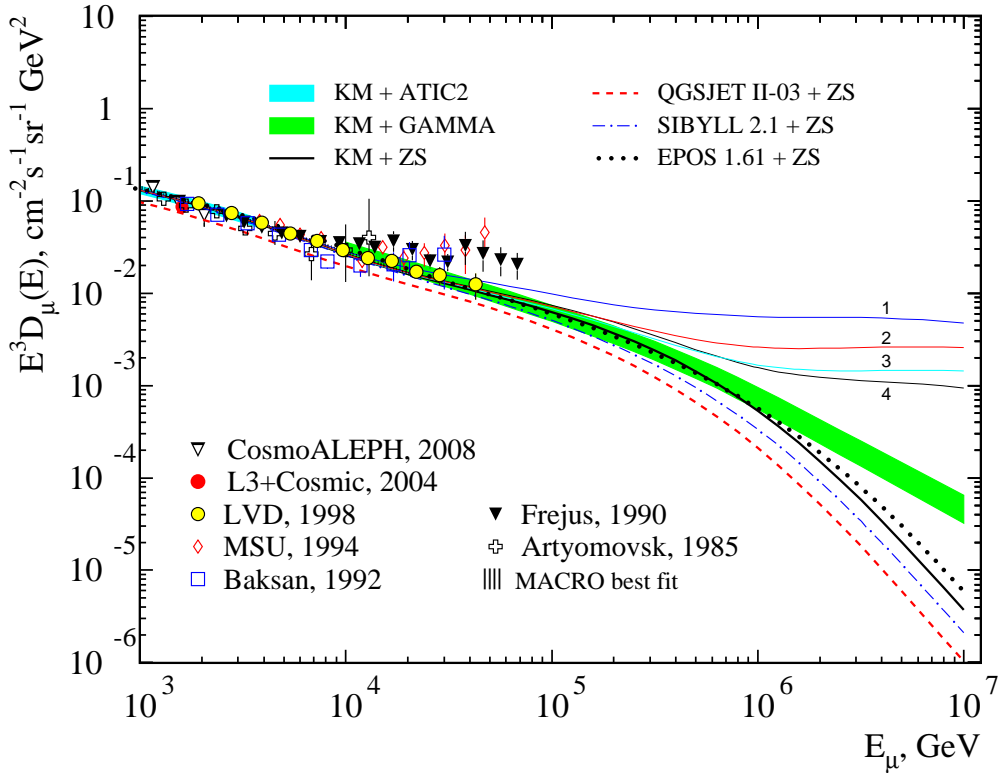


Fig. 2: The high energy vertical muon spectra at ground level. The dashed-line curves and shaded areas present this work calculations with the ATIC-2 primary spectrum [17] ($E_\mu < 10$ TeV) and GAMMA one ($E_\mu > 10$ TeV). The solid curve mark the computation for the primary spectrum model by Zatsepin and Sokolskaya [19]. The numbers near thin lines indicate the prompt muon flux model: 1 - RQPM [12], 2 and 3 – the two calculation versions of PRS [23], 4 – QGSM [12], [13].

into account the prompt muon component (thin lines in Fig. 2). While, the LVD data are well described.

The ZS model seems to be a reasonable bridge from TeV energy range to PeV one, providing a junction of the different energy ranges. Above 10^6 GeV the muon flux is apparently affected by the primary cosmic ray ambiguity in the vicinity of ‘knee’.

IV. MUON CHARGE RATIO

The muon charge ratio depends on the proton to neutron ratio in primary cosmic rays as well as on the hadron production cross-sections. Thus, a comparison of the calculated μ^+/μ^- ratio with experimental data in a wide energy range gives a possibility to study indirectly these features. At present time the muon charge ratio is measured with new facilities, that supply with high quality data from large number of muon events at high energies.

In Fig. 3 we present our calculations of μ^+/μ^- ratio along with the data of experiments [24], [25], [32], [33], [34], [35], [36], [37], [38], [39], [40], [41]. The calculations are made with the three hadronic interaction models and the two primary cosmic ray spectra. Solid line and dashed one mark the KM + GH computation for the zenith angles 0° and 90° , thin line indicates the KM + ZS result at 0° . Bold dotted line indicates the

SIBYLL 2.1 + GH result, dotted shows the QGSJET-II + GH one, both for 0° . One may see that the KM and SIBYLL calculations reproduce data well with both versions of the primary spectra, GH and ZS. The calculated curves correspond approximately to the value 1.3, that is in agreement with the recent data of BESS-TeV, CosmoALEPH, and L3+Cosmic experiments up to 1 TeV. For higher energies the kaon source of muons becomes more intensive leading to a maximum of the muon ratio, ~ 1.4 , at energy close to 10 TeV. This value agrees with the recent results of the MINOS far detector [39]. The calculations also are in agreement with the spectrograph MUTRON data [35] at $\theta = 89^\circ$ including the point above 10 TeV.

The QGSJET-II model (lower line) shows visible deviation from others: the predicted μ^+/μ^- ratio is close to ~ 1.2 , that might be explained by the higher extent of the proton and neutron flux equalization in the atmosphere due to reactions $pA \rightarrow nX$ in the model (see Fig. 1).

V. CONCLUSIONS

One may expect that the primary cosmic ray uncertainty beyond the ‘knee’ would be negligible, if real prompt muons at energies around $\sim 10^6$ GeV (Fig. 2) would appear at the flux level that not to be much lower

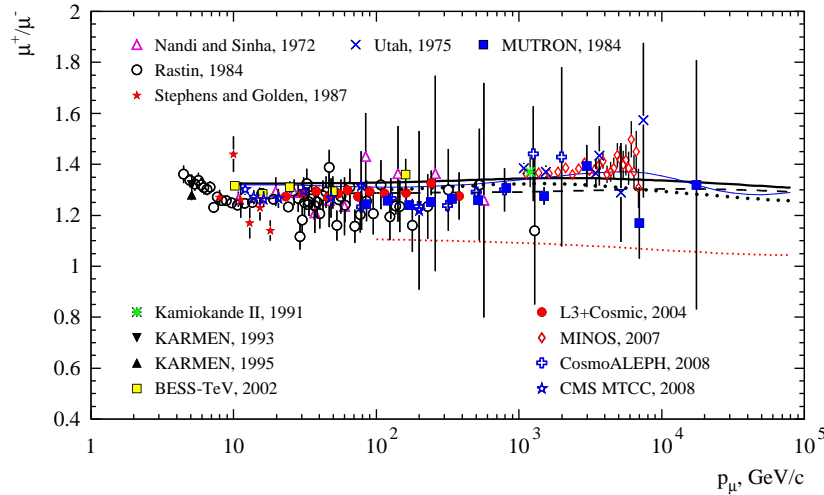


Fig. 3: Muon charge ratio at ground level computed for the three hadronic interaction models and the two primary cosmic ray spectra. Solid line marks the KM + GH result for $\theta = 0^\circ$, dashed line shows the same at 90° . Thin line: the KM + ZS at 0° , bold-dotted: the SIBYLL 2.1 + GH, dotted (the lower): the QGSJET-II + GH at 0° .

than the QGSM prediction.

It seems reasonable to consider that the prompt muon flux higher than it is predicted by RQPM, is excluded [3]. One may expect that more strong restriction of the prompt muon flux range will be extracted from the experiment in the near future.

ACKNOWLEDGEMENTS

We are grateful to T. Pierog for clarifying comments concerning codes of the hadronic interaction models. This research was partly supported in part by the Russian Federation Ministry of Education and Science within the programme "Development of Scientific Potential in Higher Schools" under grants 2.2.1.1/1483, 2.1.1/1539 and by Federal programme "Russian Scientific Schools", grant NSh-1027.2008.2.

REFERENCES

- [1] V. Aynutdinov et al., *Astropart. Phys.* 25, 140 (2006)
- [2] V. Aynutdinov et al., *Nucl. Instrum. Meth. A* 588, 99 (2008)
- [3] A. Achterberg et al. (IceCube Collaboration), *Phys. Rev. D* 76, 042008 (2007)
- [4] M. Ackermann et al., *ApJ* 675, 1014 (2008)
- [5] P. Berghaus for the IceCube Collaboration, Muons in IceCube, arXiv:0902.0021v1 [astro-ph.HE]
- [6] S. S. Ostapchenko, *Nucl. Phys. B (Proc. Suppl.)* 151, 143 (2006); S. Ostapchenko, *Phys. Rev. D* 74, 014026 (2006)
- [7] R. S. Fletcher et al., *Phys. Rev. D* 50, 5710 (1994); R. Engel et al. Proc. 26th ICRC, Salt Lake City, 1999, vol. 1, p. 415
- [8] K. Werner, T. Pierog, AIP Conf. Proc. 928, 111 (2007); astro-ph/0707.3330; T. Pierog, K. Werner, in: Proc. 30th ICRC, Merida, HE.1.6, No.905, 2007; K. Werner, *Nucl. Phys. B (Proc. Suppl.)* 175-176, 81 (2008)
- [9] A. N. Kalinovsky, N. V. Mokhov, Yu. P. Nikitin, Passage of high-energy particles through matter, AIP, New York, 1989
- [10] A. A. Kochanov et al., Proc. 30 ICRC, Universidad Nacional Auto'noma de Me'xico, Mexico City, Mexico, 2008. Vol. 5. P. 1511-1514; astro-ph/0706.4389
- [11] A. A. Kochanov, T. S. Sinigovskaya, S. I. Sinigovsky, *Astropart. Phys.* 30, 219 (2008); axXiv:0803.2943v2 [astro-ph]
- [12] E. V. Bugaev et al., *Nuovo Cim. C* 12, 41 (1989)
- [13] E. V. Bugaev et al., *Phys. Rev. D* 58, 054001 (1998)
- [14] A. Misaki et al., *J. Phys. G* 29, 387 (2003)
- [15] R. Enberg, M. H. Reno, I. Sarcevic, *Phys. Rev. D* 78, 043005 (2008)
- [16] V. A. Naumov, T. S. Sinigovskaya, *Phys. Atom. Nucl.* 63, 1927 (2000)
- [17] A. D. Panov et al., *Bull. Russ. Acad. Sci. Phys.* 71, 494 (2007); astro-ph/0612377
- [18] A. P. Garyaka et al., *Astropart. Phys.* 28, 169 (2007)
- [19] V. I. Zatsepin, N. V. Sokolskaya, *Astron. Astrophys.* 458, 1 (2006); *Astron. Lett.* 33, 25 (2007)
- [20] T. Antoni et al., *Astropart. Phys.* 24, 1 (2005); W. D. Apel et al., *Astropart. Phys.* 31, 86 (2009)
- [21] T. K. Gaisser et al. Proc. 27th ICRC, Hamburg, 2001, vol. 1, p. 1643; T. K. Gaisser, M. Honda, *Annu. Rev. Nucl. Part. Sci.* 52, 153 (2002)
- [22] A. B. Kaidalov, O. I. Piskunova, *Sov. J. Nucl. Phys.* 41, 816 (1985); *Sov. J. Nucl. Phys.* 43, 994 (1986); *Z. Phys. C* 30, 145 (1986); O. I. Piskunova, *Sov. J. Nucl. Phys.* 56, 1094 (1993)
- [23] L. Pasquali, M. H. Reno, I. Sarcevic, *Phys. Rev. D* 59, 034020 (1999)
- [24] P. Achard et al., *Phys. Lett. B* 598, 15 (2004)
- [25] C. Grupen, *Nucl. Phys. B (Proc. Suppl.)* 175-176, 286 (2008); N. Omar Hashim, CERN-THESIS-2007-047
- [26] G. T. Zatsepin et al., *Izv. Ross. Akad. Nauk. Fiz.* 58, 119 (1994)
- [27] M. Ambrosio et al., *Phys. Rev. D* 52, 3793 (1995)
- [28] M. Aglietta et al., *Phys. Rev. D* 58, 092005 (1998)
- [29] W. Rhode, *Nucl. Phys. B (Proc. Suppl.)* 35, 250 (1994)
- [30] V. N. Bakatanov et al., *Yad. Fiz.* 55, 2107 (1992)
- [31] R. I. Enikeev et al., *Yad. Fiz.* 47, 1044 (1988)
- [32] S. Haino et al., *Phys. Lett. B* 594, 35 (2004)
- [33] B. C. Nandi, M. S. Sinha, *J. Phys. A* 5, 1384 (1972)
- [34] G. K. Ashley, J. W. Keuffel, M. O. Larson, *Phys. Rev. D* 12, 20 (1975)
- [35] S. Matsuno et al., *Phys. Rev. D* 29, 1 (1984)
- [36] B. C. Rastin, *J. Phys. G* 10, 1629 (1984)
- [37] S. A. Stephens, R. L. Golden, Proc. 20th ICRC, Moscow, vol. 6, 1987, p. 173
- [38] T. E. Jannakos, FZKA Report 5520 (Forschungszentrum Karlsruhe, 1995)
- [39] P. Adamson et al., *Phys. Rev. D* 76, 052003 (2007)
- [40] M. Yamada et al., *Phys. Rev. D* 44, 617 (1991)
- [41] M. Aldaya, P. Garcia-Abia, CMS NOTE-2008/016, CERN Document Server: <http://cdsweb.cern.ch>